

Combined opto-impedimetric whole-cell biosensors for environmental applications

Trinh Quang Thong^{1*}, Nguyen Quang Dich^{2*}, Trieu Viet Phuong³, Gerald Gerlach⁴

¹ Faculty of Engineering Physics (FEP)

² The Institute of Control and Automation Technology (ICEA)

Hanoi University of Science and Technology (HUST), Hanoi, Vietnam

³ Vietnam National Standard and Quality Institute (VSQI), Hanoi, Vietnam

⁴ Institute of Solid State Electronics (IFE), Dresden University of Technology (TUD), Dresden, Germany

*Corresponding author E-mail: thong.trinhquang@hust.edu.vn, dich.nguyenquang@hust.edu.vn

DOI: <https://doi.org/10.64032/mca.v29i4.330>

Abstract

Environmental pollution is the big concern of people in developing countries like Vietnam. In this scope, electrochemical sensors based on impedance technique have proved to be a promising method due to their portability, rapidity, sensitivity, low cost, ease of miniaturization, and label-free operation that can be used for on-the-spot detection. In this work, the design and fabrication of the whole-cell sensors for the environmental and food-safety applications were implemented. The sensor structure consists of a glass plate with two coated transparent ITO (indium tin oxide) microelectrode arrays and four-compartment micro-fluidic cell. The electrode structure is in the form of 24 inter-digitated fingers so-called comb-structure with a length of 11 mm and 0.5 μ m in width. The living cells are integrated into sensor structure for the evaluation of use biological effect of analytic substance. The sensor's detection principle is based on the changes in impedance combined with fluorescent signals via the operation of the microfluidic cell. The sensor was tested for the detection of diclofenac concentrations between 10 and 100 μ M in nutrient medium. The obtained results show the obvious changes in output signals for both of impedance and fluorescence characterization of the investigated samples.

Keywords: whole cell biosensor, PDMS microfluidics, fluorescent protein, Diclofenac

Symbols

Symbols	Units	Description
Z	Ω	Impedance
I	A	Opto-electrical current

Abbreviations

PCB	Print Circuit Board
ITO	Indium-Tin Oxide
PDMS	Polydimethylsiloxane
LED	Light Emitting Diode
CMOS	Complementary Metal-Oxide Semiconductor
NSAID	Non-Steroidal Anti-inflammatory Drug
DAQ	Data Acquisition
WCBs	Whole-Cell Biosensors

1. Introduction

Like other developing countries, Vietnam also have the environmental problems including air polutions caused by the exhaust gases from vehicles and factories, waste chemicals from industry, agriculture, and products for life that all can harm the human's health. One of those causes is the waste of used pharmaceutical products like antibiotics and palliatives which can enter the soil and water sources and consequently the human body via employing the foods and drinking water. In this scenario, using biosensors is considered a scientific way to detect and quantitatively measure the agents causing the environmental pollution.

Traditionally, for indicating or detecting the presence of toxicants in environmental pollution, the chemical methods using gas chromatography-mass or liquid spectrometry are usually used [1-8]. The analytical methods can be carried out precisely with relatively good sensitivity. However, those are time consuming and expensive because it is necessary to transport the samples to the laboratory and requires special equipped laboratories. During the past time, many studies of using biosensors, of which are whole-cell biosensors (WCBs) have been implemented to monitor the pollutant [9-15] because of their advantages like portability, compact, good sensitivity, and low cost based on the advanced technology. Particularly, biosensors can detect very small amounts of chemicals or biological samples like virus, bacteria, and even cells or/and ADN. For this purpose, the biological components like enzymes, antibodies, and microorganisms can be used in sensors' structure. Whole cells deployed in biosensor systems can be considered one of the practical successes of molecular-scale devices. WCBs based on microbial cells are easy to genetically modify and inexpensive since large quantities can be produced and beyond only the bioavailable portion of the analyte detect. Methods for immobilizing enzymes to be detected in a membrane or gelmatrix have been developed to construct biosensors. Recently, new whole-cell biosensors have been developed that the mechanism for detection can be the electrochemical means. These promoter-based, whole-cell biosensors are suitable for online and in situ monitoring of pollutants [16-21].

Existing WCBs may face several limitations, including sensitivity to analyte concentration, limitations in dynamic range and robustness, long detection times, high detection

limits, and dependence on specific reporter gene selection and molecular recognition elements. Normally, the WCBs provide signal from complex electrode systems using layers, surfaces, or membranes where electrical charge transfer and ion diffusion processes take place. However, there is also a challenge of sensor's sensitivity, which depends on the thickness of the sensing layer. Too thin sensing layer would decrease the signal to noise ratio leading to the decrease in sensitivity. Too thick sensing layer would reduce the detected AC impedance current that the electron transfer between layers is hindered and the sensitivity is also decreased. Here, proposed opto-impedimetric sensors can overcome these issues by leveraging the advantages of electrical impedance measurements. In this circumstance, the fluorescent protein as the reporter was developed to identify sensitive biomarkers for environmental toxicity [22 - 27]. It is because, fluorescence detection can recognize the response of an electrochemical cell to a voltage at different frequencies. Therefore, a coupled change in fluorescence intensity signal can be considered an alternative solution to improve the sensor sensitivity and extend its linear working.

This paper focuses on description of a design of the combined optical-impedimetric sensors with a readout circuit for both impedance and fluorescence signal. The sensors can be realized by using simple fabrication and assembly process. The sensor system including electrical and optical module was tested to detect the residual concentrations of diclofenac in environment after use. It is a NSAID used to treat pains associated with gout, sprains of muscles and joints and in mild to moderate fever in some cases. After being orally used the drug's residue that may reaches up a concentration 70 at % is excreted via the urine in the wastewater cycle considered a problem of environmental pollution. The fact is known that the uptake of those substances can lead to harmful effects of free-living species and in particular underwater creatures like fishes, shrimps, crabs, consequently the problems to human health.

2. Sensor design and measurement setup

2.1 Sensor design

The main structure of the sensor system consists of an electrical module for impedance measurement as shown in Figure 1. In order to evaluate the change in output signal from the device, the module has two arrays of micro-interdigitated electrodes for independent measurements symmetrically designed, serving as the measuring and referent channels with 12 couples of fingers for each (Figure 1a). The reason of using micro-interdigitated electrodes (IDEs) is that IDEs offer significant advantages over traditional electrode configurations, particularly in sensor applications. Their comb-like structure, with closely spaced so-called "fingers" results in the enhanced performance in several key areas.

Firstly, IDEs structure allows to control the signal strength by easily changing its dimension, a wide frequency spectrum of use, and low energy consumption of the capacitive transduction mechanism, very compactness with high contact and effective sensing area, maximizing the interaction between the electrode surface and the analyte. Secondly, the close proximity of the electrode fingers enables reducing

diffusion distances that minimizes the diffusion path length for analytes, leading to quicker ion diffusion and faster response times, and consequently, a better signal-to-noise ratio.

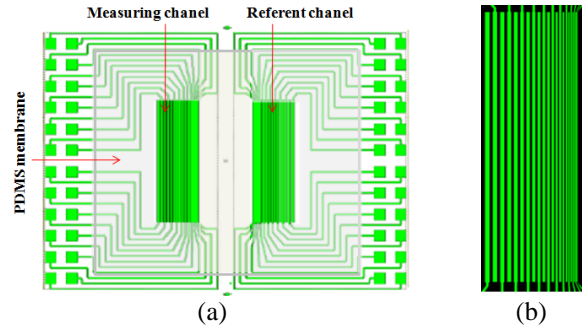


Figure 1: Design of impedance sensor (a) and electrode configuration for measuring and referent channel (b).

The structure enables to increases significantly the effective capacitance of the device, making it more sensitive to changes in dielectric properties caused by analyte binding. Lastly, IDEs structure can more effectively confine the electric field within the sensing layer, leading to a more localized and sensitive interaction with the analyte. The IDEs structure is also convenient to amplify signals, improve detection limits, and provide cost-effective and robust solutions compared to traditional electrode configurations. In this design, the dimension of one finger is 11 mm in length and 0.5 μ m in width. Particularly, both the finger's width and gap between the fingers were designed to vary from 5 μ m to 186 μ m and 2.5 μ m to 133.5 μ m, respectively. This design allows the penetration depth of the electric field into the medium which is convenient for measurement implemented by Sciospec ISX-3v2 impedance spectrometer.

2.2 Sensor fabrication and measurement setup

The sensor was fabricated by CMOS technology using only one photomask which was designed by Corel Draw software as shown in Figure 2.

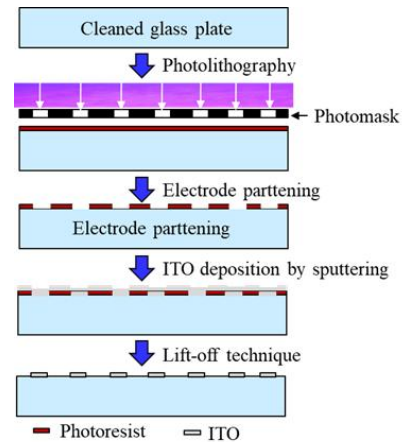


Figure 2: Fabrication process of sensor's structure

Firstly, the glass plate having dimension of 34 mm x 28 mm x 1 mm were cleaned, successively, in acetone and isopropanol, then dried by purity N₂ gas. The electrode structure was patterned on the glass plates. Next, a thin film of ITO was deposited on by RF magnetron sputtering using a

2" sintered target made by a blend of In_2O_3 and SnO_2 with a weight ratio 9:1. The deposition rate was 0.16 nm/min corresponding to the RF power of 20 W. After that, it was a post-deposition thermal treatment that ITO films were annealed at 100 °C for 4 hours in a quartz tubular furnace having an oxygen flow with a pressure of 2×10^{-1} Pa. Finally, ITO electrode structure was realized by lift-off technique.

Two micro-fluidic cells are mounted on measuring and referent windows (Figure 3).

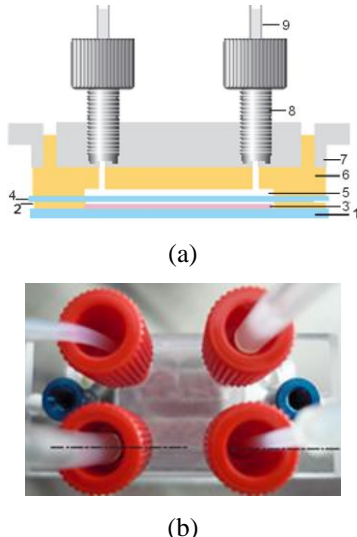


Figure 3: Sensor assembly (a) and image of tubes providing detected and reference solution (b)

(1 - glass plate with coated ITO electrodes; 2 - PDMS membrane; 3 - hydrogel with fluorescent cells in the lower chamber; 4 - porous polycarbonate membrane; 5 - upper chamber in PDMS; 6 - upper PDMS part with the fluid microchannels; 7 - microfluidic connections; 8 - screw; 9 - 1/16" tubes)

This part is made of polycarbonate (PC) for passing the analyte solution. The upper chambers are separated from the lower chambers by thin oxyphene porous membrane which contains pores with a diameter of 1 μm , allows the diffusion of nutrients and analyte to the investigated cells and preventing the passage of cells (diameter about 5 microns). A lower chamber and an upper chamber above form a measuring and reference channel as shown in Figure 3a. Each channel is connected to a pump by means of the screws and tubes illustrated in Figure 3b.

The measurement and referent chamber for comparison of output signal were formed by using a 500 μm thick PDMS membrane having dimension of 21.5 mm x 21.5 mm with two opened windows of 5 mm x 15 mm, precisely placed on the coated ITO electrode arrays (Fig. 1b). In this scenario, PDMS is a versatile silicone elastomer which is optical transparency, biocompatibility and low-cost fabrication, and widely used in engineering and biomedical applications. These characteristics have made PDMS a natural choice for microfluidic devices. PDMS's flexibility and ability to replicate complex geometries have promoted the progress of the research in the field of biosensors. After pressing the PDMS film against the glass plate, the openings forming two lower chambers of the microfluidic cell are filled with a hydrogel containing the fluorescent yeast cells.

The implemented optical module shown in (Figure 4) contains two LED rows that can emit the green fluorescent with wavelengths between 485 nm and 510 nm. Herein, an integrated and diminutive fluorescence detector with high

sensitivity is used that a high-power LED for exciting and a photodiode (PD) for acquiring fluorescence signals. The PDMS film is covered with a porous polycarbonate membrane (Oxyphen AG, Unique-Mem® Track-Etched Membrane, 20 μm thick, 1 μm pore diameter). A current-light dual circuit was designed to achieve a stable excitation light, and the signal-noise ratio was improved by amplifying and filtering the fluorescence signal at the detection side. The small sensitive area of detection allows a very significant improvement in signal/noise ratio that supports the disadvantage of fluorescence detection. Fig. 4b is the readout circuit for stimulation and measurement of the fluorescence signal as well a current-to-voltage converter based on an operational amplifier which was developed by CiS Research Institute for Micro Sensors, an institution in the fields of micro sensor and microsystems technology in Germany. In the combination of opto-impedimetric measurement, the fluorescence signal was detected when switching on either one LED row or two LED rows (470 nm, 27 V, 8 mA).

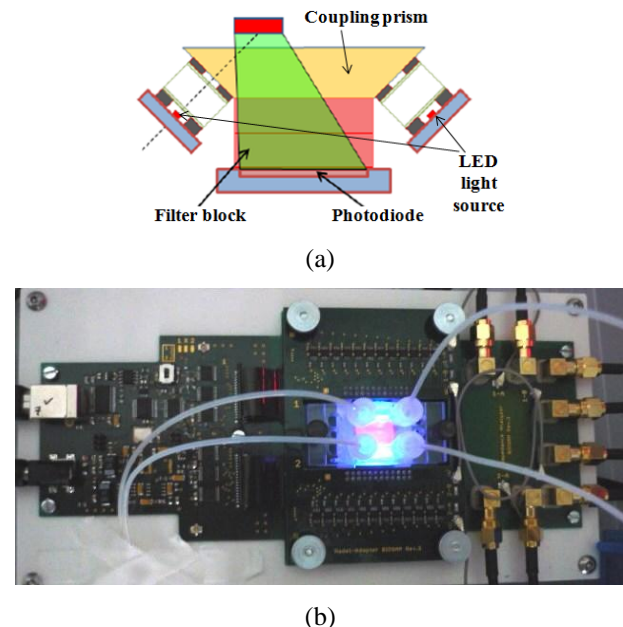


Figure 4: Model of sensor's optical module (a) and well sited device under test (b)

After all, the optical and electrode module, and microfluidic cell are fixed on the PCB board of readout circuit of which the measuring principle is illustrated by a diagram shown in Figure 5a. The electrical contacting of the ITO microelectrode arrays is effected by spring contacts. The fluorescence signal was detected using a photodiode with a matched built-in filter. The photocurrent was measured by means of a current-voltage converter based on an OP177 operational amplifier, and by means of a LabJack U3 or U6 Pro card and monitored inline with the software DAQ FactoryExpress or LabVIEW. The fluorescence spectrum was recorded on a USB2000 spectrometer (Ocean Optics Inc.), which provides absorbance, transmission, reflectance, and radiation measurements, and evaluated with appropriate SpectraSuite software. The overall picture of the measurement system in study is presented in Figure 5b. Three replications for each serially diluted concentration in the 10-100 μM range were tested over several consecutive days to cut down the change in diclofenac concentration by time.

The means and standard deviations of the impedance magnitude were examined in the frequency range between 10 Hz and 1MHz. The differences between means was determined based on a one-way analysis of variance having a significance in excess of 95% (or $P < 0.05$). The lower detection limit of the sensor was set corresponding to the measured diclofenac concentration with a mean impedance value significantly different from the blank.

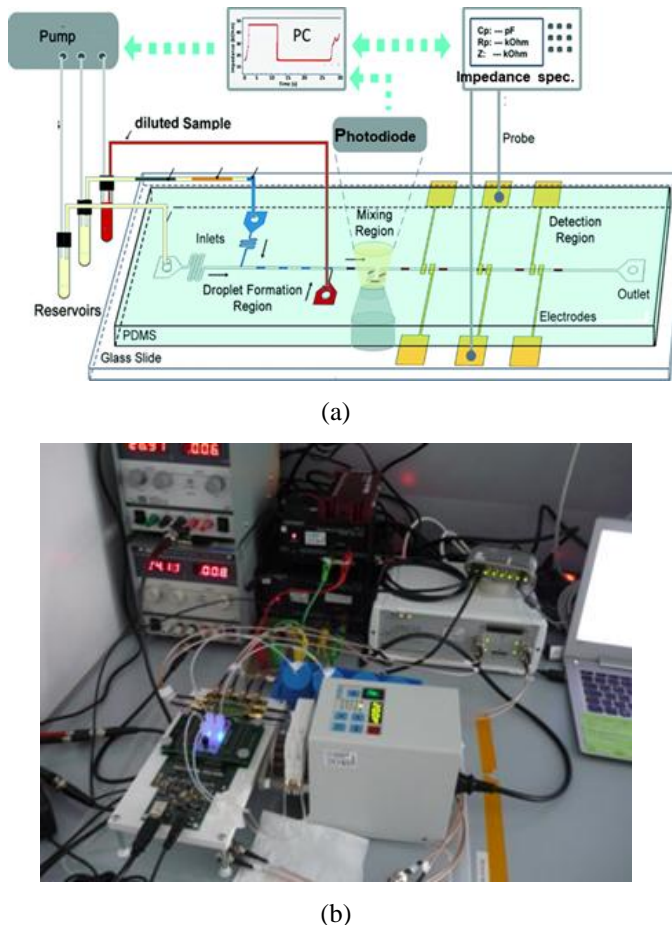


Figure 5: Experimental setup: exploded diagram (a) and real overview of measurement system (b)

3. Results and discussion

Test measurements were carried out for diclofenac concentration diclofenac in waste water. For measurements with living cells, one of the two chambers served as a reference with only the nutrient medium flowing through it. In this circumstance the enzyme used here is yeast cells *Saccharomyces cerevisiae* BY4741 p426PDR5-tGFP. The cell is immobilized via its diffusion process into the polymerized hydrogels which are mixtures based on hydroxypropyl methacrylate (HPMA), 2-(dimethylamino)ethyl methacrylate (DMAEMA), tetraethylene glycol dimethacrylate (TEGDMA) and ethylene glycol (EG). The immobilized gel is put in the medium of 1 μ M diclofenac solution. The presence of diclofenac cells affects the measuring impedimetric signal by their electrical properties. The measurement results of impedance spectroscopy with so-called Bode diagrams are plotted by

graph demonstrating the frequency-dependent impedance amount IZI. The results of the impedance measurements are shown in Figure 6 and 7. Here, Figure 6 compares the spectra for the cells immobilized in gel and for the cell suspended on the ITO electrode arrays in a microfluidic cell. Meanwhile, Figure 7 focuses in detail the change in the impedance modulus at a frequency of 100 kHz for immobilized cells in the medium and in 1 μ M diclofenac solution. The time-dependent impedance increase was caused by the cell proliferation due to the swelling of DMEMA hydrogel of which swelling kinetics and characteristics have been systematically investigated in previous works [28-32]. This result confirms the impedance spectrum depending on the electrode configuration. It means that the sensor design demonstrated well the purpose of using the device for bio-applications.

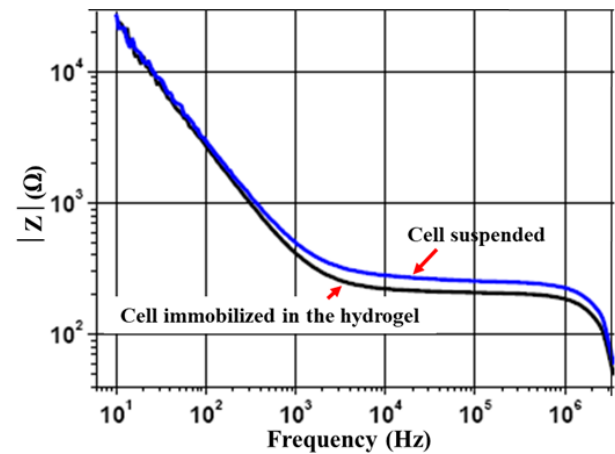


Figure 6: Impedance spectra for the immobilized and suspended cell

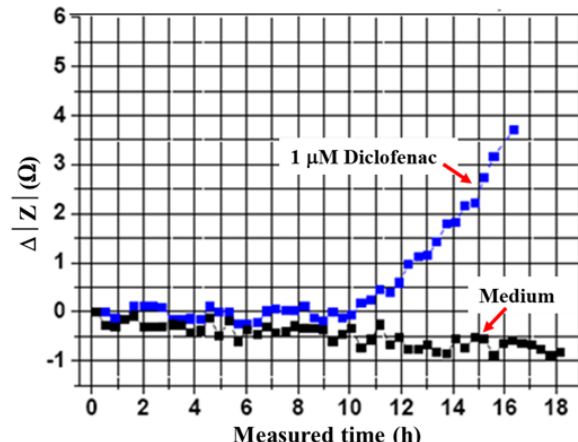


Figure 7: Change in the impedance modulus at a frequency of 100 kHz for immobilized cells in the medium and in 1 μ M diclofenac solution

As shown in Figure 6, the impedance magnitude $|Z|$ significantly changes with the investigated range of frequency. The measured result shows the distinct impedance spectra for immobilized cells versus cell suspension. That is the impedance spectrum varies depending on whether the cells are immobilized in a gel or suspended in a microfluidic cell. Both conditions generally show a decrease in impedance as frequency increases, but their magnitudes and the rate of change with frequency differ, which can be attributed to the electrical properties of the cells and their interaction with the immobilization matrix. A cell can be described by an

equivalent circuit diagram where its membrane is represented by two capacitances and its interior by an ohmic resistor. Herein, the impedance depends on both frequency and diclofenac concentration. At frequency over 1 MHz, there is little change in impedance with respect to diclofenac concentration because the impedance is largely dominated by dielectric capacitance of the sample media. It means that at high frequency, the effect of bacteria bound to the sensor surface is minimized due to the relaxation of small dipole species (water molecules). It is because the impedance caused by the double layer capacitance and the parasitic capacitance which is minimized at high frequencies. Figure 7 demonstrates the time-dependent change in impedance ($\Delta|Z|$) that increases for immobilized cells exposed to a 1 μM diclofenac solution, compared to cells in the medium alone. In this circumstance, the behavior of electrodes and transport processes can be modeled by components like Warburg impedance, charge transfer resistance, and double-layer capacitance, all of which exhibit frequency-dependent characteristic. Clearly, the impedance increase is directly attributed to cell proliferation induced by the diclofenac. This indicates that at each specific frequency, like 100 kHz, the biological response (cell proliferation) can be captured to the presence of the analyte (diclofenac) via impedance changes.

In addition, the obtained results of impedance measurement directly demonstrates the sensor's capability to detect diclofenac at a concentration of 1 μM considered the limit of detection (LOD). A distinct and time-dependent increase in the impedance modulus is observed for immobilized yeast cells exposed to 1 μM diclofenac solution, in contrast to cells in the medium alone. The clear differentiation indicates that 1 μM is within the sensor's detection capabilities for impedimetric measurements, at least over time. This correlation between the impedance change and a biological response (cell proliferation) provides a strong indication of the sensor's accuracy in identifying the effect of diclofenac showing a reliable and specific response to the analyte. This result can be considered a sensor's detection limit for impedimetric component.

The photodiode current was determined by means of a current-voltage transducer based on a operational amplifier. The optical signal was determined by the fluorescence module which was located below the micro-fluidic cell with immobilized cells. Figure 8 shows the change in the photodiode current as a function of the diclofenac concentration for 16 hours overflow with MM (minimal medium nutrient solution), mixed with different diclofenac concentrations.

This result is summed up relying on the recorded signal from two measured regimes each of which is corresponding to a light emitted by every LED for in-turn channels of measurement and referent ones. The expected linear function of this characterization indicates that the fluorescent proteins embedded in the hydrogels respond very well with the excited lights emitted from the LED of optical module. The provided graphs illustrate the photodiode current as a function of diclofenac concentration ranging from 0 to 50 μM , after a 16-hour exposure. For sensor's LOD, the optical signal consistently increases with diclofenac concentration, showing a clear trend from the lowest tested non-zero concentrations up to 50 μM . In fact, for low concentrations, it might yield

less "obvious" changes, implying that the optimal or reliably quantifiable range for fluorescence detection should start from 10 μM . The linearity suggests that the optical detection method provides accurate and proportional measurements of diclofenac concentrations within the investigated range (0-50 μM) which contributes to the overall accuracy of the optical readout.

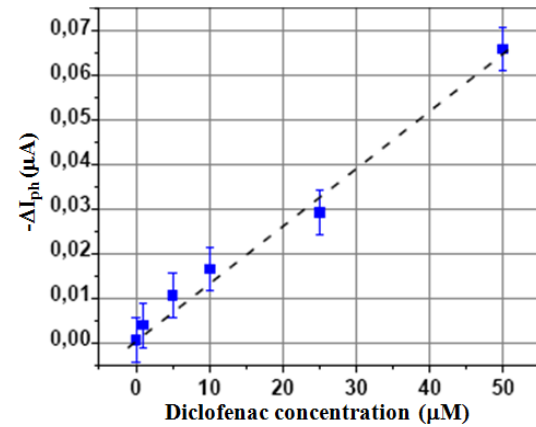


Figure 8: Photodiode current as a function of the diclofenac concentration

4. Conclusion

In this contribution, we present our study of a novel combined optical-impedance biosensor for the application of monitoring the environmental pollution. The sensor design was successfully realized by a simple fabrication and assembly process providing a complex module that is convenient for simultaneous monitoring of optical and impedimetric signals. The sensor output characterizations show the accepted trends for detecting the objects to be defined. Namely, in the measurement test, the present of diclofenac concentration in water was found clearly by using the sensor and measurement setup. Unlike traditional analytical methods like gas chromatography-mass spectrometry (GC-MS) or liquid chromatography-mass spectrometry (LC-MS), which are precise but time-consuming, expensive, and require specialized laboratories and staff, this biosensor is designed to be inexpensive and suitable for on-site measurements. This aligns with the general advantages of whole-cell biosensors, which offer portability, rapidity, and lower costs. The development was driven by the need to detect diclofenac, a persistent pharmaceutical pollutant, in wastewater for the fast detection of small amounts of solutes. In conclusion, this combined opto-impedimetric whole-cell biosensor for diclofenac is unique in its dual readout capability, providing both specific analyte detection and general cell health monitoring. It represents an advancement in providing inexpensive, on-site, and on-line detection solutions, fitting well within the broader trend of practical WCBs applications. While its detection limits are in the micromolar range, which is higher than some highly optimized WCBs for other specific targets.

In the future, such sensors can be miniaturized and are on-line capable based on micro-electro-mechanical system (MEMS) technology by which both the IDEs structure and

optical components could be integrated on a chip. It means that another sensor design and fabrication process could be provided. For the practice, with further development of the cells towards improved sensitivity, such a sensor system could be used to detect the residual pesticide in water and fruits that now becomes a serious problem of environmental pollution and food safety in Vietnam.

Acknowledgement

The authors would like to thank the colleagues of IFE, TU Dresden, Germany for their collaboration to provide the read-out circuit for detection of sensor output signals.

References

- [1] Casper, H. H., McMahon, T. L., Paulson, G. D. (1985) Capillary gas chromatographic-mass spectrometric determination of fluoroacetate residues in animal tissues, *J. Assoc. Off. Anal. Chem.*, 68: 722-725.
- [2] Ross M.M., Kidwell D.A. and Callahan J.H. (1989) Mass-spectrometric analysis of anatoxin-a., *J. Analyt. Toxicol.*, 13 (6): 317-312
- [3] Himberg, K., (1989) Determination of anatoxin-a, the neurotoxin of Anabaena flos-aqua cyanobacterium, in algae and water by gas chromatography-mass spectrometry, *J. Chromatog.*, 481: 358-362
- [4] Harada, K.-I., et al. (1993) Liquid chromatography/mass spectrometric detection of anatoxin-a, a neurotoxin from cyanobacteria, *Tetrahedron*, 49: 9251-9260
- [5] Lawton L.A., Edwards C. and Codd G.A. (1994) Extraction and high-performance liquid chromatographic method for the determination of microcystins in raw and treated waters, *Analyst*, 119: 1525-1530.
- [6] Locke S.J. and Thibault P. (1994) Improvement in detection limits for the determination of paralytic shellfish poisoning toxins in shellfish tissues using capillary electrophoresis/electrospray mass spectrometry and discontinuous buffer systems. *Analyst. Chem.*, 66: 3436-3446.
- [7] Lawrence, J.F., Menard, C. and Cleroux, C. (1995) Evaluation of pre-chromatographic oxidation for liquid chromatographic determination of paralytic shellfish poisons in shellfish. *J. AOAC Int.*, 78: 514-520.
- [8] Harada K.-I., Murata H., Qiang Z., Suzuki M. and Kondo F. (1996) Mass spectrometric screening method for microcystins in cyanobacteria. *Toxicon*, 34: 701-710.
- [9] Scott DL, Ramanathan S, Shi W, Rosen BP, Daunert S. (1997) Genetically engineered bacteria: electrochemical sensing systems for antimonic acid and arsenite. *Anal Chem*, 69:16-20.
- [10] Biran I, Babai R, Levcov K, Rishpon J, Ron EZ (2000) Online and in situ monitoring of environmental pollutants: electrochemical biosensing of cadmium, *Environ Microbiol*, 2: 285-290.
- [11] Bontidean I, Mortari A, Leth S, Brown NL, Karlson U, Larsen MM, Vangvonsveld J, Corbisier P, Csoregi E (2004) Biosensors for detection of mercury in contaminated soils. *Environ Pollut*, 131:255-262.
- [12] Leedjärv A, Ivask A, Virta M, Kahru A (2006) Analysis of bioavailable phenols from natural samples by recombinant luminescent bacterial sensors. *Chemosphere*, 64:1910-1919.
- [13] Lee JH, Mitchell RJ, Kim BC, Cullen DC, Gu MB (2005) A cell array biosensor for environmental toxicity analysis. *Biosens Bioelectron*, 21:500-507.
- [14] Popovtzer R, Neufeld T, Biran D, Ron EZ, Rishpon J, Shacham-Diamond Y (2005) Novel integrated electrochemical nano-biochip for toxicity detection in water. *Nano Lett*, 5:1023-1027.
- [15] Lee JH, Gu MB (2005) An integrated mini biosensor system for continuous water toxicity monitoring. *Biosens Bioelectron*, 20:1744-1749.
- [16] Bousse, L., Whole cell biosensors. *Sensors and Actuators B: Chemical*, 34(1-3), (1996), pp. 270–275. doi:10.1016/s0925-4005(96)01906-5.
- [17] Kovacs, G. T. A., Electronic sensors with living cellular components, *Proceedings of the IEEE*, 91(6), (2003), pp. 915–929. doi:10.1109/jproc.2003.813580.
- [18] Paitan Y, Biran I, Shechter N, Biran D, Rishpon J, Ron EZ (2004) Monitoring aromatic hydrocarbons by whole cell electrochemical biosensors. *Anal Biochem*, 335: 175-183.
- [19] Chouteau C, Dzyadevych S, Durrieu C, Chovelon JM (2005) A bi-enzymatic whole cell conductometric biosensor for heavy metal ions and pesticides detection in water samples. *Biosens Bioelectron*, 21:273-281.
- [20] Gu MB, Mitchell RJ, Kim BC (2004) Whole-cell-based biosensors for environmental biomonitoring and application. *Adv Biochem Eng Biotechnol*, 87:269-305.
- [21] Daunert S, Barret G, Feliciano JS, Shetty RS, Shrestha S, Smith WA (2001) Genetically engineered whole-cell sensing systems: coupling biological recognition with reporter genes. *Chem Rev*, 12:2705-2738.
- [22] Kohler S, Belkin S, Schmid RD (2000) Reporter gene bioassays in environmental analysis. *Fresenius J Anal Chem*, 366:769-779.
- [23] Simpson ML, Sayler GS, Applegate BM, Ripp S, Nivens DE, Paulus MJ, Jellison GEJ (1998) Bioluminescent-bioreporter integrated circuits from novel whole-cell biosensors. *Trends Biotechnol*, 16:332-338.
- [24] Farre M, Goncalves C, Lacorte S, Barcelo D, Alpendurada MF (2002) Pesticide toxicity assessment using an electrochemical biosensor with *Pseudomonas putida* and a bioluminescence inhibition assay with *Vibrio fischeri*. *Anal Bioanal Chem*, 373:696-703.
- [25] Shetty RS, Deo SK, Liu Y, Daunert S (2004) Fluorescence-based sensing system for copper using genetically engineered living yeast cells. *Bio-technol Bioeng*, 88:664-670
- [26] Pedahzur R, Polyak B, Marks RS, Belkin S (2004) Water toxicity detection by a panel of stress-responsive luminescent bacteria. *J Appl Toxicol*, 24:343-348.
- [27] Ulrike Schmidt, Carola Jorsch, Margarita Guenther, and Gerald Gerlach (2016) Biochemical piezoresistive sensors based on hydrogels for biotechnology and medical applications, *J. Sens. Sens. Syst.*, 5: 409-417.
- [28] Kimberly Cook-Chennault, Sharmad Anaoka, Alejandra M Medina Vázquez, Mizan Chennault, Influence of High Strain Dynamic Loading on HEMA–DMAEMA Hydrogel Storage Modulus and Time Dependence, *Polymers*, 16(13), 2024, 1797. doi: 10.3390/polym 16131797.
- [29] Chen Yanfeng, Yi Min, Swelling kinetics and stimuli-responsiveness of poly(DMAEMA) hydrogels prepared by UV-irradiation Radiation Physics and Chemistry, 61 (2001), pp. 65–68. DOI: 10.1016/S0969-806X(00)00374-1.
- [30] Simone Villani, Renata Adami, Ernesto Reverchon, Anna Maria Ferretti, Alessandro Ponti, Marilena Lepretti, Ivana Caputo & Lorella Izzo, pH-sensitive polymersomes: controlling swelling via copolymer structure and chemical composition, *Journal of Drug Targeting*, 2017. DOI: 10.1080/1061186X.2017.1363216.
- [31] Roko Blažić, Dajana Kucić Grgić, Marijana Kraljić Roković, Elvira Vidočić, Cellulose-g-poly(2-(dimethylamino)ethylmethacrylate) Hydrogels: Synthesis, Characterization, Antibacterial Testing and Polymer Electrolyte Application, *Gels*, 7;8(10), 2022, 636. doi: 10.3390/gels8100636.
- [32] Fulya Taktaka and Yasasin Ogen, Preparation and characterization of novel silk fibroin/2-(N,N-dimethylamino)ethyl methacrylate based composite hydrogels with enhanced mechanical properties for controlled release of cefixime, *Journal of Macromolecular Science, Part A*, 54:7 (2017), pp. 458-464, DOI: 10.1080/10601325.2017.1320750.